MEASUREMENT OF FIBER DEPOSITION IN A HUMAN LUNG MODEL BY PHASE CONTRAST MICROSCOPY WITH AUTOMATED IMAGE ANALYSIS

František Lízal*, Jakub Elcner*, Miloslav Bělka*, Jan Jedelský*, Philip K. Hopke†, Pavel Štarha‡, Hana Druckmüllerová‡, Miroslav Jícha*

Deposition of fibers in human lungs is known as a health hazard. In-vitro measurements were performed with glass fibers in a realistic model of human lungs up to the seventh generation of branching to estimate the effect of fiber size and breathing pattern on fiber deposition. Deposited fibers were rinsed from the model segments and gathered on nitrocellulose filters. Phase-contrast microscopy with high resolution camera was used to capture images of filters with fibers. New software was developed for an automated image analysis and local deposition characteristics were calculated afterwards. The whole method proved to be a useful and valuable tool for the evaluation of fiber and particle deposition.

Keywords: *fiber deposition, phase contrast microscopy, image analysis*

1. Introduction

Fiber is an elongated particle, usually defined by the ratio of the length to the diameter over 3 [1]. Inhalation of fibers is known as notorious health hazard. Research was conducted especially on asbestos fibers, but also man-made vitreous fibers (MMVFs), often used as a substitute for asbestos, has raised the concerns of the potential health hazards [2]. Each asbestos fiber size was found to be related to different diseases. Fibers 0.15 to 3 μm in diameter and 2 to 100 μm long are associated with asbestosis (scarring of lung tissue), fibers less than 0.1 μm in diameter and 5 to 100 μm long with mesothelioma (cancer of the lining of the lung), and fibers 0.15 to 3 μm in diameter and 10 to 100 μm long with lung cancer [3].

Few experimental works have been performed to characterize the deposition pattern of fibers. Su and Cheng [4] used carbon fibers and performed experiments with constant inspiratory flowrates between 15 and 60 l/min on a human airway replica consisting of the oral cavity and following airways up to the fourth bifurcation. Their results proved that most high-inertia fibers were deposited in the oropharynx and the carina ridges of bifurcations. The following comparison [5] with small momentum fibers (TiO_2 and glass) showed that only very few small momentum fibers were deposited in the airway cast. It means they can easily penetrate the upper airway and have a pathogenic effect in the lower airways. Numerical simulation of Zhang et al. [6] implies that lower deposition efficiency of fibers in

* Ing. F. Lízal, Ph.D., Ing. J. Elcner, Ing. M. Bělka, doc. Ing. J. Jedelský, Ph.D., prof. Ing. M. Jícha, CSc., Brno University of Technology, Faculty of Mechanical Engineering, Energy Institute, Technická 2, Brno

† prof. P. K. Hopke, Center for Air Resources Engineering and Science, Clarkson University, 8 Clarkson Ave. Potsdam, New York, USA

‡ Ing. P. Štarha, Ph.D., Ing. H. Druckmüllerová, Brno University of Technology, Faculty of Mechanical Engineering, Institute of Mathematics, Technická 2, Brno

comparison with spherical particles is probably caused by tendency of fibers to align with the air flow.

It is necessary to perform more experiments in realistic models of airways to ascertain potential harmful effects of glass fibers, often used in building industry as insulation. Therefore, a realistic segmented model up to the eighth bifurcation [7] was used for the measurement with glass fibers.

2. Methods

The model consists of oral cavity and following airways up to eighth bifurcation (see Fig. 1). The model is segmented and thus allows easy evaluation of local deposition characteristics.

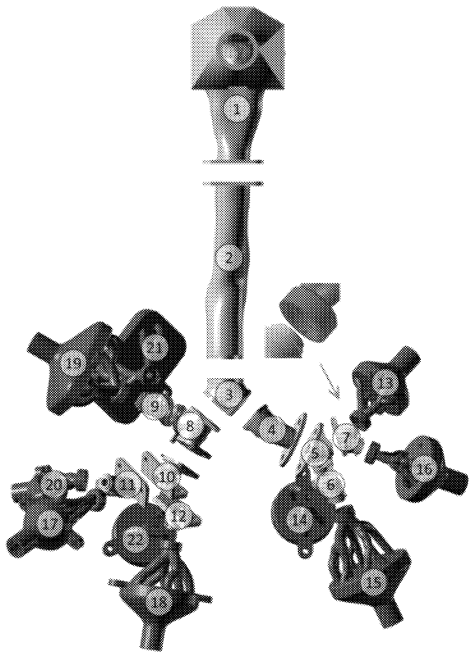

Fig.1: The realistic model of human lungs and numbering of its segments

The experimental setup (Fig. 2) consists of a fiber generation system, a classifier, a humidifier, a dilutor, the model of lungs with ten outputs, ten filters and flowmeters (each connected to one model output), and a vacuum pump. The complete description of the fiber generation and classification system was published by Wang et al [8]. Concisely, the glass fibers with the average diameter 1 μm and density 2.56 g/cm3 were dispersed to the air, humidified, their electrical charge was removed by ^{210}Po ionizing unit and they were classified according to their length. The fibers coming out from the classifier had narrow length distribution with count average length 10.1 μm and standard deviation 1.2 μm.

They were mixed with air in the dilutor to achieve homogenous aerosol with flowrate 30 l/min, which corresponds to steady inspiration during deep breathing. The inner surface of the model was coated with silicone oil to simulate mucous layer and to prevent bouncing of fibers from the wall. The aerosol flew through the model and non-depositing particles were

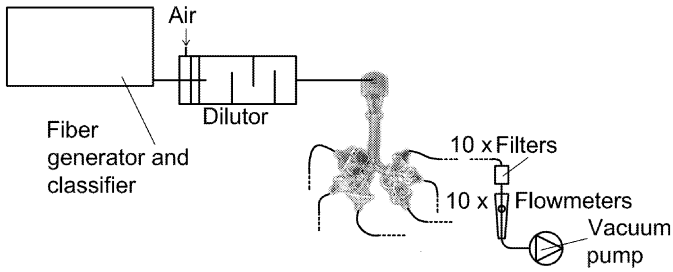

Fig.2: The simplified scheme of the experimental setup

collected behind the model outputs on nitrocellulose membrane filters. The flow through the outputs of the model was controlled by flowmeter valves to simulate realistic conditions.

Subsequent analysis of fiber deposition was based on a modified PCM (Phase-Contrast Microscopy) method for counting fibers [1]. The model was disassembled into segments and each segment was put into a beaker with isopropanol and sonicated to release the fibers into the solvent. Isopropanol with fibers was then filtrated through nitrocellulose filters. Filters with deposited fibers were dried in a dustless environment. After that the filters were mounted on a microscope slide and rendered transparent using acetone vapors. These filters are hereafter denoted as *rinse filters*.

Filters used for collecting fibers after each output of the model were directly placed on the microscope slide and also rendered transparent. These filters are hereafter denoted as output filters. Phase-contrast microscopy enables visualization of transparent glass fibers deposited on a transparent filter and mounted on a transparent microscope slide due to phase shift of the light passing through a fiber in a sample. The phase shift is visualized using interference with a non-shifted reference beam.

The classical PCM method [1] for counting fibers is based on a manual optical counting, which is time consuming and demands high attention of a microscopist. Despite maximal effort of the microscopist, the result still tends to be influenced by subjective conditions of the person, such as health state, experience, current mood or ambient environment conditions. Therefore a following modification of the method was employed. High resolution gray scale imaging of the filters was made using a camera Atik 320 E mounted on a microscope with phase contrast (Nikon Eclipse), and novel software was developed for identification and counting of the fibers in images.

The image analysis consists of six main steps; the results of each step are presented in Fig. 3. The original image (Fig. 3a) is down-scaled, a median filter is applied on the result to remove the fibers, and then the image is rescaled back to the original resolution using iterative bilinear interpolation with the scale factor 1.5 (Fig. 3b) to create an artificial background image. The calibration is performed by dividing the original image by the image of the background (Fig. 3c). The next step is the Adaptive Contrast Control method (ACC), which enhances fine details (Fig. 3d). The noise reduction is done by means of a linear filter with rotating Gaussian kernel (Fig. 3e). The following image shows the image being split into the identified objects and the background (Fig. 3f). The fibers differ from other objects in size and shape. First, small objects are removed. Then, the shape of the potential fibers is analyzed and objects that are not elongated enough are removed (Fig. 3g). The last step is the analysis of identified fibers (Fig. 3h). However, the automated analysis is applicable only on high quality images. If the image contains excessive number of non-fibrous objects,

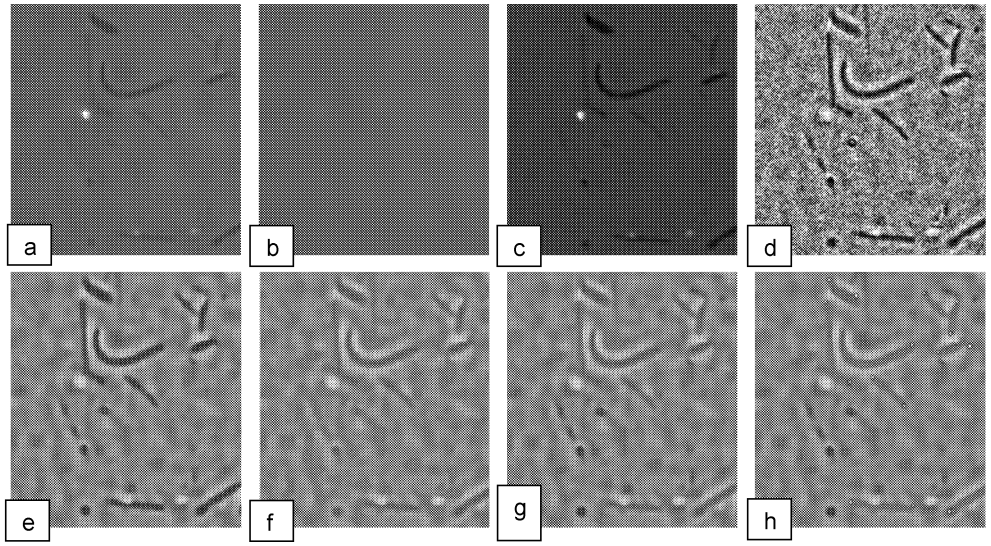

Fig.3: Procedure of the automated analysis : a) original image, b) background, c) calibrated image, d) application of Adaptive Contrast Control method, e) rotating Gaussian kernel, f) threshold method segmentation, g) removal of non-fiber objects, h) analysis of fiber ending

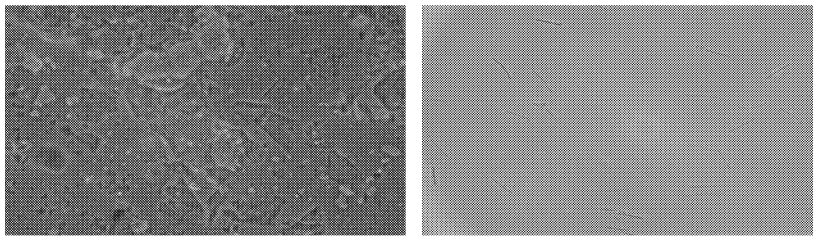

Fig.4: Images of rinse (left) and output (right) filters

the software is not capable to distinguish between fibers and other objects. In our case, the filters which contained fibers rinsed from the segments of the model (Fig. 4 left) were of worse quality and had to be counted manually, despite the known disadvantages of the method. Prior to the evaluations of the experiments, the automated and manual methods of fiber counting were applied on a testing set of samples, the results were compared and compatibility of both methods was verified.

An important task for the future set of experiments is to ensure the highest possible quality of rinse filters in order to allow automated analysis of all the filters from the experiment. There are 32 rinse filters and 40 to 80 output filters (depending on the duration of aerosol exposition) from each experiment. Output filters must be changed every 30–60 minutes to prevent overfill of the filter.

3. Results and discussion

Results acquired by both the automated and manual methods of counting were verified on a set of 10 sample filters (Fig. 5). The Average relative difference of counts was 11.1 %, which is acceptable considering the repeatability and variability of the classical PCM method [1].

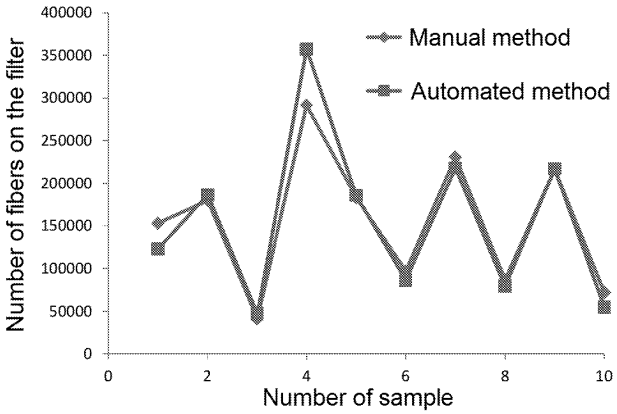

Fig.5: Comparison of Manual and automated method of counting

Main deposition characteristics were calculated from the data. *Deposition fraction* is a ratio of the number of fibers deposited in a given segment to the number of fibers entering the model. *Deposition efficiency* is a ratio of the number of fibers deposited in a given segment to the number of fibers entering the segment. *Deposition density* is a ratio of the deposition fraction in the segment to the inner surface area of the segment. Error bars represent the maximal difference which was found between two experiments in any segment.

Output filters are denoted by numbers 23–32 in Fig. 6. There is a significant difference between output filters and other segments in deposition fraction, but an almost negligible difference can be found between the individual segments. As can be seen from the deposition efficiency chart (Fig. 7), the lowest deposition efficiency was measured on the first three segments and on segment eight, which is connected to segment three (please see Fig. 1). This is confirmed also by the deposition density chart (Fig. 8). It means the effect of fiber alignment in the flow has the maximal effect in the upper part of the airways.

Two experiments for a steady inhalation regime with a flow rate of 30 l/min are presented in Fig. 9. Stokes number used for comparison of deposition of different particles in different

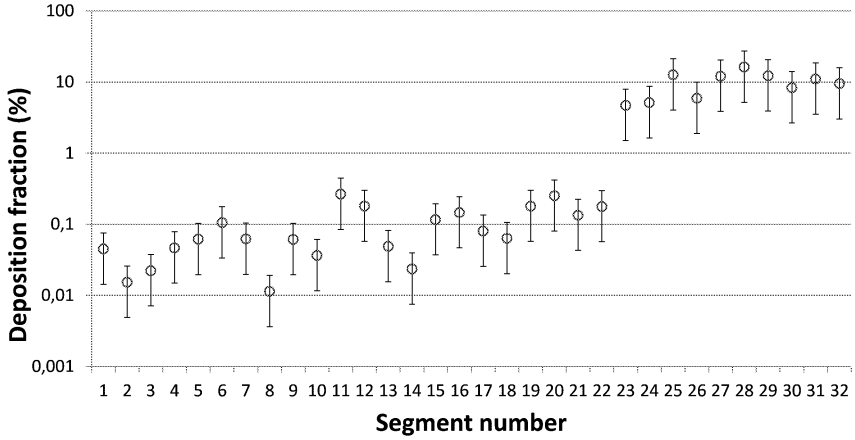

Fig.6: Deposition fraction, segment numbers correspond to Fig.1

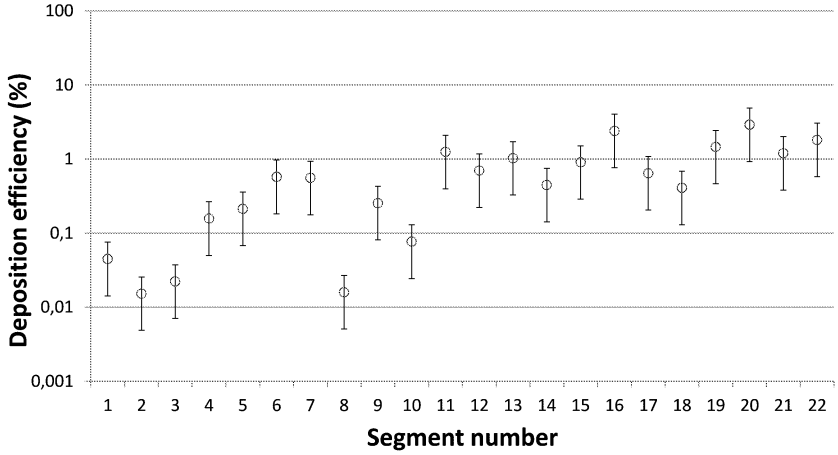

Fig.7: Deposition efficiency, segment numbers correspond to Fig.1

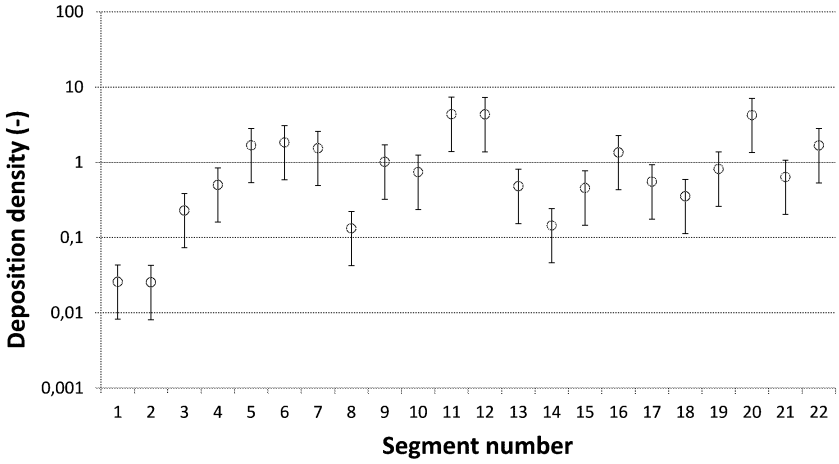

Fig.8: Deposition density, segment numbers correspond to Fig.1

lung models was calculated on the basis of aerodynamic diameter d_{ae} according to [4]

$$d_{\mathrm{ae}} = d_{\mathrm{ve}} \sqrt{\frac{\varrho}{\varrho_0\, \kappa_{\mathrm{r}}}} \tag{1}$$

where d_{ve} is volume equivalent diameter, ϱ is density of fiber, ϱ_0 is density of water and κ_{r} is dynamic shape factor for randomly oriented prolate spheroid, which is calculated from the dynamic shape factor for prolate spheroid parallel κ_{p} and perpendicular κ_{k} to the direction of the flow. β is a ratio of fiber length to the diameter.

$$\kappa_{\mathrm{k}} = \frac{\dfrac{8}{3}\,(\beta^2-1)\,\beta^{-1/3}}{\dfrac{2\,\beta^2-3}{\sqrt{\beta^2-1}}\,\ln\!\left(\beta-\sqrt{\beta^2-1}\right)+\beta}\,, \tag{2}$$

$$\kappa_{\mathrm{p}} = \frac{\dfrac{4}{3}\left(\beta^2 - 1\right)\beta^{-1/3}}{\dfrac{2\,\beta^2 - 3}{\sqrt{\beta^2 - 1}}\,\ln\left(\beta - \sqrt{\beta^2 - 1}\right) - \beta}\ , \tag{3}$$

$$\frac{1}{\kappa_{\mathrm{r}}} = \frac{1}{3\,\kappa_{\mathrm{p}}} + \frac{2}{3\,\kappa_{\mathrm{k}}}\ . \tag{4}$$

The Stokes number is then given by

$$\mathrm{Stk} = \frac{\varrho_0\, d_{\mathrm{ae}}\, U_{\mathrm{s}}}{18\,\eta\, D} \tag{5}$$

where U_{s} is the mean velocity in the parent tube of the bifurcation, η is the air viscosity and D is the mean diameter of the parent tube of the bifurcation.

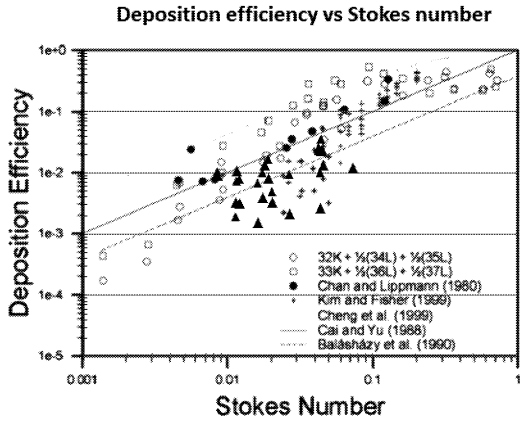

Fig.9: Comparison of deposition of fibers with deposition of spherical particles published by Zhou and Cheng [9]; our data are represented by black triangles; (modified from [9])

A Comparison of our data for fibers with previously published deposition of spherical particles (Fig. 9) demonstrated that the deposition of fibers is lower than the deposition of spherical particles [9]. Therefore fibers can penetrate deeper into the lungs.

4. Summary

A novel approach was applied to evaluation of fiber deposition in the model of human lungs. The glass fibers were rinsed from the model and deposited on nitrocellulose membrane filters. Fibers passing through the model were collected on output filters during the experiment. All filters were rendered transparent and filters with sufficient quality were scanned by high-resolution camera. Images were then processed by special algorithms and deposited fiber counts were exported. The automated analysis means saving time and provides unbiased results. This advantage would be even more noticeable in connection with automated traversing mechanism of the microscope stage with the sample. The computational analysis also allows measurement of fiber diameter, length and can contain statistical analysis of the data measured. However, high quality filters are necessary for application of the automated image analysis.

Rinse filters were of worse quality due to the presence of impurities and had to be counted manually. The compatibility of the results acquired by both the automated and manual methods of counting was verified on a set of 10 sample filters. The resulting numbers of fibers in particular segments were transformed to deposition characteristics. The calculated deposition efficiency was compared to data for spherical particles published previously. Lower deposition of fibers in comparison to spherical particles is induced by their tendency to direct themselves in the flow direction. Future experiments will be focused on the influence of different breathing regimes and different lengths of fibers with maximal effort to achieve high quality filters suitable for the automated analysis.

Acknowledgement

This work was supported by the project FSI-J-11-36/1344.

References

[1] World Health Organization (WHO), Determination of airborne fibre number concentrations, A recommended method by phase-contrast optical microscopy (membrane filter method), Geneva: WHO, 1997, 53 p.

[2] Cavallo D., Campopiano A., Cardinali G., Casciardi S., de Simone P., Kovacs D., Perniconi B., Spagnoli G., Ursini C.L., Fanizza C.: Cytotoxic and oxidative effects induced by man-made vitreous fibers (MMVFs) in a human mesothelial cell line, Toxicology, Sep 2004, vol. 201, no. 1–3, p. 219–229

[3] Hinds W.C.: Aerosol technology : properties, behavior, and measurement of airborne particles, New York: Wiley, 1999, 483 p., ISBN 0471194107

[4] Su W.C., Cheng Y.S.: Deposition of fiber in a human airway replica, Journal of Aerosol Science, Nov 2006, vol. 37, no. 11, p. 1429–1441

[5] Su W.C., Cheng Y.S.: Deposition of man-made fibers in human respiratory airway casts, Journal of Aerosol Science, Mar 2009, vol. 40, no. 3, p. 270–284

[6] Zhang L., Asgharian B., Anjilvel S.: Inertial and interceptional deposition of fibers in a bifurcating airway, J Aerosol Med, 1996, vol. 9, no. 3, p. 419–430

[7] Lizal F., Elcner J., Hopke P.K., Jedelsky J., Jicha M.: Development of a realistic human airway model, Proceedings of the Institution of Mechanical Engineers Part H-Journal of Engineering in Medicine, 2012, vol. 226, no. H3, p. 197–207

[8] Wang Z.C., Hopke P.K., Baron P.A., Ahmadi G., Cheng Y.S., Deye G., Su W.C.: Fiber classification and the influence of average air humidity, Aerosol Science and Technology, Nov 2005, vol. 39, no. 11, p. 1056–1063.

[9] Zhou Y., Cheng Y.S.: Particle deposition in a cast of human tracheobronchial airways, Aerosol Science and Technology, Jun 2005, vol. 39, no. 6, p. 492–500

Received in editor's office: October 15, 2012
Approved for publishing: April 18, 2013